

## Multiuser Decorrelating Based Long-Range Frequency-Domain Channel Transfer Function Prediction in Multicarrier DS-CDMA Systems

Bin Hu, Wei Liu, Lie-Liang Yang and Lajos Hanzo  
School of ECS, University of Southampton, SO17 1BJ, UK.

Tel: +44-23-8059 3125, Fax: +44-23-8059 4508

Email: bh202r,wl03r,lly,lh@ecs.soton.ac.uk; http://www-mobile.ecs.soton.ac.uk

**Abstract**— In this contribution, multiuser decorrelating based frequency-domain channel estimation and long range channel prediction techniques are proposed for a generalized Multicarrier DS-CDMA (MC DS-CDMA) system communicating over a fast fading and frequency-selective channel. In the MC DS-CDMA system considered, the channel transfer function (CTF) is estimated in the frequency-domain with the aid of pilot symbols by invoking the multiuser decorrelating based channel estimation technique, in order to reduce the effects of both the Multiuser Interference (MUI) and the background noise. Then, Kalman filter assisted long-range channel prediction is carried out with the aid of both the current and previous frequency-domain CTFs for the sake of predicting the future CTFs. Furthermore, a sinc-interpolator is employed for the sake of deriving the frequency-domain CTFs associated with the data symbols. Our simulation results show that for a reasonable signal-to-noise ratio (SNR) value the proposed frequency-domain multiuser decorrelating based channel estimator is robust to the effects of both the MUI as well as the noise.

### I. INTRODUCTION

One of the most challenging problems in high data rate wireless systems is that of overcoming the effects of dispersion imposed by multipath propagation. Based on a combination of Direct Sequence Code Division Multiple Access (DS-SS) and Orthogonal Frequency Division Multiplexing (OFDM), MC DS-SS [1], [2], [3], [4], [5], has been proposed for a variety of high-rate wireless communication applications. In this contribution, we discuss the generalized MC DS-SS system investigated in [6], which incorporates the subclasses of both multitone DS-SS [3] and orthogonal MC DS-SS [4] as special cases. In the MC DS-SS system considered, the entire frequency band is divided into a number of subcarriers. Signals transmitted in each subcarrier experience flat fading, provided that the bandwidth of each subcarrier is lower than the coherence bandwidth of the channel. Moreover, a sufficient long cyclic prefix can be incorporated for the sake of compensating for both the asynchronous delay differences of the different users as well as for the delay-spread-induced inter-symbol interference (ISI) imposed by the dispersive channel [2]. In this case, each of the subcarriers can be estimated or predicted using a variety of schemes designed for flat fading channels.

On the other hand, in future wireless systems, the carrier frequency is likely to be high, which results in normalized high Doppler frequencies. Thus, using the outdated channel transfer function (CTF) estimated based on the past received data using Decision Directed Channel Estimation (DDCE) principles [2] may not be sufficiently accurate. However, with the aid of long range CTF prediction, the future Channel Impulse Response (CIR) or CTF may be estimated sufficiently accurately [7]. Various algorithms have been proposed in the literature [7], [8], [9], [10], [11] for the sake of implementing long range CIR or

The financial support of the European Union under the auspices of the Phoenix and Newcom projects and that of the EPSRC,UK is gratefully acknowledged.

CTF prediction. In [7], the CIR was predicted based on the Minimum Mean Square Error (MMSE) estimation principles. The most important characteristic of this algorithm is that the sampling rate is typically significantly lower than the data rate. In [8] the ROOT-MUSIC algorithm was invoked for non-dispersive channel envelope prediction. By contrast, the ESPRIT algorithm was employed for the prediction of fast-fading wideband channels in [9]. Furthermore, in [10], [11] both the one-dimensional 1-D and 2-D Unitary-ESPRIT algorithms have been employed for estimating the CTF. Once the CTF has been determined, its future values can be extrapolated in both the time and frequency domain using the techniques proposed in Chapters 15 and 16 of [2].

*By contrast, the novelty of this paper is that we invoke the multiuser decorrelating based channel estimation scheme in the context of generalized MC DS-SS for the sake of estimating the frequency-domain (FD) CTF while reducing the effects of both the Multiuser Interference (MUI) and the background noise. Then, Kalman filter assisted long range FDCTF prediction is carried out in order to predict the future CTFs based on both the current and previous CTFs determined with the aid of the dedicated MC DS-SS pilot symbols to be described in Section III. Finally, we generate the frequency-domain CTFs associated with the data symbols by employing a sinc interpolator.*

The rest of this paper is organized as follows. In Section II the philosophy of the uplink generalized Multicarrier DS-SS system and the wideband wireless channel are briefly described. In Section III the multiuser decorrelating based channel estimation scheme is investigated, while the long range channel predictor assisted by both a Kalman filter and a sinc-interpolator are considered in Section IV. The attainable performance is studied in Section V. Finally, Section VI offers our conclusions.

### II. SYSTEM MODELS

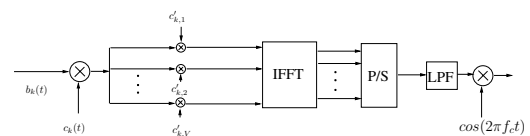


Fig. 1. Transmitter schematic of MC DS-SS using both time-domain and frequency-domain spreading

The transmitter of the generalized MC DS-SS system is portrayed in Fig.1. At the transmitter side, the binary data stream  $b_k(t)$  is spread using an  $N$ -chip time domain DS spreading waveform  $c_k(t)$ . The DS spread signals are simultaneously modulated using Binary Phase Shift Keying (BPSK) and then spread using a frequency domain orthogonal spreading sequence  $\mathbf{c}'_k = [c'_{k,1}, c'_{k,2}, \dots, c'_{k,V}]$  of length  $V$ , where we have  $\mathbf{c}'_k \cdot \mathbf{c}'_k^H = 1$ . In our investigations we

assume that OFDM using  $V$  subcarriers was invoked [2], where  $V$  consecutive chips of the MC DS-CDMA spreading sequences were mapped to  $V$  different subcarriers during an OFDM symbol and hence the OFDM symbol duration was  $T_c = T_b/N$ . The spread OFDM chip-vector of  $V$  subcarriers can be expressed as  $\mathbf{s}_k = \mathbf{c}'_k b_k c_k(t) = [s_1, s_2, \dots, s_V]$ . The Inverse Fast Fourier Transform (IFFT) is then invoked for modulating the  $V$  subcarriers by using the spread OFDM chip-vector  $\mathbf{s}_k$  [2]. The output signal of the IFFT-based demodulator is a block of  $V$  number of time domain samples in parallel form. After parallel to serial (P/S) conversion these time domain signals are transmitted through a multipath fading channel, which is assumed to have  $L$  paths.

In our investigations, block-based data transmission is considered where there are  $M$  useful MC DS-CDMA symbols, namely  $[b_{k,0j}, b_{k,1j}, \dots, b_{k,(M-1)j}]$ , in  $j$ th block. Thus the  $k$ th user's  $j$ th transmitted signal block after IFFT and P/S conversion can be expressed as  $[\tilde{s}_{k,0j}, \tilde{s}_{k,1j}, \dots, \tilde{s}_{k,(M-1)j}]$ , where the chip-vector  $\tilde{\mathbf{s}}_{k,mj}$  represents the IFFT of the spread OFDM chip-vector  $\mathbf{s}_{k,mj}$ , which can be expressed as

$$\mathbf{s}_{k,mj} = \mathbf{c}'_k b_{k,mj} c_k(t). \quad (1)$$

A cyclic prefix of length  $L$  is inserted in the chip-vector  $\tilde{\mathbf{s}}_{k,mj}$  prior to transmission for the sake of compensating for both the asynchronous delay differences of the different users as well as for the delay-spread-induced ISI imposed by the dispersive channel [2]. Furthermore, a guard interval of length  $\tau_{max}$  is inserted in each transmission block for the sake of preventing the inter-symbol-block-interference among different users, where  $\tau_{max}$  is the maximum delay of all users, which is normalized to the OFDM symbol period  $T_c = T_b/N$ . Consequently, a transmission block is comprised of  $\{(V+L-1)NM + \tau_{max}V\}$  chips and hence the duration of a transmission block  $T_B$  may be expressed as  $T_B = \{(V+L-1)NM + \tau_{max}V\} \cdot T_{c'}$ , where  $T_{c'} = \frac{T_b}{NV}$  is the chip-duration.

We assume that the CIR encountered is time-invariant during a transmission block [12]. Therefore, the CIR corresponding to the  $j$ th transmission block can be expressed as:

$$h_{kj}(t) = \sum_{\ell=0}^{L-1} h_{kj,\ell} \cdot \delta(t - \tau_{k,\ell} T_{c'}), \quad (2)$$

where  $h_{kj,\ell}$  is the complex channel gain experienced by the signal of the  $k$ th user in the  $\ell$ th path, which obeys Rayleigh fading, while  $\tau_{k,\ell}$  is the  $k$ th user's delay in the  $\ell$ th path. Let us assume that the first user corresponding to  $k = 1$  is the user-of-interest and his/her delay is  $\tau_{k,0} = 0$  for simplicity.

At the receiver, the TD samples of the received signal corresponding to the cyclic prefix are first removed and  $V$ -point FFT is invoked for demodulating the remaining  $V$  samples and generating the demodulated subcarrier signals in the FD [2]. Consequently, the received signal can be expressed in vectorial form as  $\mathbf{r}_{mj} = [r_{mj,0}, r_{mj,2}, \dots, r_{mj,V-1}]^T$ ,

$$\mathbf{r}_{mj} = \sum_{k=1}^K \mathbf{C}'_k \mathbf{H}_{kj} b_{k,mj} c_k(t) + \mathbf{n}_{mj} = \mathbf{G}_j \mathbf{b}_{mj} + \mathbf{n}_{mj}, \quad (3)$$

where  $\mathbf{H}_{kj} = [H_{kj,0}, H_{kj,2}, \dots, H_{kj,V-1}]^T$  denotes the FDCTF, and  $\mathbf{C}'_k = \text{diag}\{\mathbf{c}'_k\}$ . The matrix  $\mathbf{G}_j$  in Eq.(3) is an  $(V \times K)$ -dimensional matrix comprising both the channel's complex-valued FD fading factors and the FD spreading signatures of all the  $K$  users,

hence we have  $\mathbf{G}_j = [\mathbf{g}_{1j}, \mathbf{g}_{2j}, \dots, \mathbf{g}_{Kj}]$ , where  $\mathbf{g}_{kj} = \mathbf{C}'_k \mathbf{H}_{kj}$ . Furthermore, the vector  $\mathbf{b}_{mj} = [b_{1,mj} c_1(t), b_{2,mj} c_2(t), \dots, b_{K,mj} c_K(t)]^T$  is the data vector and  $\mathbf{n}_{mj}$  is the Additive white Gaussian Noise (AWGN) vector associated with the covariance matrix of  $\sigma^2 \mathbf{I}_V$ , where  $\mathbf{I}_V$  denotes the  $(V \times V)$ -dimensional identity matrix. Finally, the  $(V \times MN)$ -dimensional matrix  $\mathbf{R}_j$  corresponding to the  $j$ th received signal block may be expressed as

$$\mathbf{R}_j = \mathbf{G}_j \mathbf{B}_j + \mathbf{N}_j, \quad (4)$$

where we have  $\mathbf{B}_j = [\mathbf{b}_{0j}, \mathbf{b}_{1j}, \dots, \mathbf{b}_{(M-1)j}]$  and  $\mathbf{N}_j$  is contributed by  $\mathbf{n}_{mj}$  of Eq.(3).

Since we assume that a cyclic prefix of length  $L$  was inserted, no OFDM ISI is incurred. Hence the FDCTF  $\mathbf{H}_{kj}$  in Eq.(3) can be expressed as the  $V$ -point DFT of the CIR  $\mathbf{h}_{kj} = [h_{kj,0}, \dots, h_{kj,L-1}]^T$ . More explicitly, we have  $\mathbf{H}_{kj} = \mathbf{F}_L \cdot \mathbf{h}_{kj}$ , where  $\mathbf{F}_L$  is an  $(V \times L)$ -dimensional matrix, which is given by the first  $L$  columns of the DFT matrix  $\mathbf{F}$  formulated as:

$$\mathbf{F} = \begin{pmatrix} 1 & 1 & \dots & 1 \\ 1 & e^{-j2\pi/V} & \dots & e^{-j2\pi(V-1)/V} \\ \vdots & \vdots & \ddots & \vdots \\ 1 & e^{-j2\pi(V-1)/V} & \dots & e^{-j2\pi(V-1)(V-1)/V} \end{pmatrix}. \quad (5)$$

### III. CHANNEL ESTIMATION

Pilot-aided channel estimation in OFDM/MC DS-CDMA systems may be carried out either by including appropriately spaced pilot subcarriers in all symbols as in [2], or by transmitting dedicated OFDM/MC DS-CDMA symbols containing no data-bearing subcarriers, followed by a number of dedicated data symbols having no pilot subcarriers [13]. In this contribution the latter technique is used. In order to mitigate the effects of both the MUI and the background noise imposed on the FDCTF prediction, channel estimation is typically carried out prior to channel prediction [7]. In [14] multiuser decorrelating technique was first proposed for signal detection in multiple user scenario. By contrast, we invoked multiuser decorrelating technique [14] in our FDCTF estimation scheme for the sake of suppressing the effects of MUI. When the pilot symbol block is received, we multiply both sides of Eq.(4) with the matrix  $\mathbf{B}_j^H (\mathbf{B}_j \mathbf{B}_j^H)^{-1}$  generated from the pilot symbols, and attain an estimate of the matrix  $\mathbf{G}_j$  encapsulating both the FDCTF  $\mathbf{H}_{kj}$  and the FD spreading signatures  $\mathbf{C}'_k$  of all the  $K$  users as follows:

$$\tilde{\mathbf{G}}_j = \mathbf{G}_j + \mathbf{N}_j \mathbf{B}_j^H (\mathbf{B}_j \mathbf{B}_j^H)^{-1} = \mathbf{G}_j + \tilde{\mathbf{N}}_j, \quad (6)$$

where  $j$  denotes the index of the received symbol blocks and  $\tilde{\mathbf{N}}_j$  is a  $(V \times K)$ -dimensional noise matrix. Consequently, the first column of the matrix  $\tilde{\mathbf{G}}_j$ , which corresponds to the desired user, is given by  $\tilde{\mathbf{g}}_{1j} = \mathbf{g}_{1j} + \hat{\mathbf{n}}_{1j}$ , where the  $(V \times 1)$ -dimensional noise vector is the first column of the noise matrix  $\tilde{\mathbf{N}}_j$ . Upon multiplying the vector  $\tilde{\mathbf{g}}_{1j}$  with the matrix  $\mathbf{C}'_1^H$ , we obtain the estimate of the desired user's FDCTF  $\mathbf{H}_{1j}$ , which can be expressed as

$$\tilde{\mathbf{H}}_{1j} = \mathbf{H}_{1j} + \mathbf{C}'_1^H \hat{\mathbf{n}}_{1j} = \mathbf{H}_{1j} + \tilde{\mathbf{n}}_{1j}, \quad (7)$$

where the vector  $\tilde{\mathbf{n}}_{1j}$  is a noise process having zero mean and a covariance of  $V \cdot \sigma^2$ . For notational convenience, the superscript and subscript denoting the reference user of  $k = 1$  will be omitted in the rest of the paper.

According to [15], the autocorrelation function of  $H_{j,v}$  can be expressed as

$$r[\Delta j; \Delta v] = E[H_{j,v} H_{j',v'}^*] = r_t[\Delta j] r_f[\Delta v], \quad (8)$$

where  $\Delta j = j - j'$ ,  $\Delta v = v - v'$ , and  $r_t[\Delta j]$  is the time-domain symbol-spaced autocorrelation function, which can be expressed as [15]

$$r_t[\Delta j] = J_0(2\pi f_{dm} \Delta j T_B), \quad (9)$$

with  $J_0(\cdot)$  representing the zero-order Bessel function of the first kind and  $f_{dm}$  denoting the maximum Doppler frequency. By contrast, the frequency-domain symbol-spaced autocorrelation function  $r_f[\Delta v]$  in Eq.(8) is given by [16]

$$r_f[\Delta v] = \sum_{\ell=0}^{L-1} \sigma_\ell^2 e^{-j2\pi \Delta v f_0 \tau_\ell}, \quad (10)$$

where we have  $f_0 = 1/(MT_b)$ , while  $\tau_\ell$  denotes the delay of the  $\ell$ th multipath component and  $\sigma_\ell^2$  is its average power. In contrast to the autocorrelation function of  $H_{j,v}$  in Eq.(8), the autocorrelation function of its estimate  $\hat{H}_{j,v}$  in Eq.(7) is given by

$$E[\hat{H}_{(j,v)} \hat{H}_{(j',v')}^*] = r_t[\Delta j] r_f[\Delta v] + V \sigma^2 \delta(\Delta j) \delta(\Delta v). \quad (11)$$

Furthermore, the cross-correlation between  $\hat{H}_{j,v}$  and  $H_{j,v}$  can be expressed as

$$E[\hat{H}_{j,v} H_{j',v'}^*] = r_t[\Delta j] r_f[\Delta v]. \quad (12)$$

Based on Eq.(7) the estimated FDCTF can be formulated as

$$\hat{\mathbf{H}}_j = \mathbf{D}_j^H \tilde{\mathbf{H}}_j, \quad (13)$$

where  $\hat{\mathbf{H}}_j$  denotes the estimate of  $\mathbf{H}_j$  and the  $(V \times V)$ -dimensional matrix  $\mathbf{D}_j = [\mathbf{d}_{j,0}, \mathbf{d}_{j,1}, \dots, \mathbf{d}_{j,V-1}]$  represents the FD coefficient matrix of the estimation filter designed for estimating  $\mathbf{H}_j$ , where  $\mathbf{d}_{j,v} = [d_{j,v,0}, d_{j,v,1}, \dots, d_{j,v,(V-1)}]^T$  is a  $(V \times 1)$ -dimensional vector. The MMSE based coefficient matrix  $\mathbf{D}_j$  may be obtained by using classic Wiener filtering, which is formulated as [17]

$$\mathbf{D}_j = \mathbf{R}_{\hat{\mathbf{H}}\hat{\mathbf{H}}}^{-1} \mathbf{R}_{\hat{\mathbf{H}}\mathbf{H}}, \quad (14)$$

where  $\mathbf{R}_{\hat{\mathbf{H}}\hat{\mathbf{H}}} = E[\hat{\mathbf{H}}_j \hat{\mathbf{H}}_j^H]$  is the  $(V \times V)$ -dimensional autocorrelation matrix of  $\hat{\mathbf{H}}_j$ , while  $\mathbf{R}_{\hat{\mathbf{H}}\mathbf{H}} = E[\hat{\mathbf{H}}_j \mathbf{H}_j^H]$  is the  $(V \times V)$ -dimensional cross-correlation matrix.

The minimum MSE (MMSE)  $J_{fo(j,v)}$  of the FDCTF estimator after FD filtering can be expressed as [17]

$$J_{fo(j,v)} = r_f[0] - \mathbf{r}_{f,v}^H \mathbf{R}_{\hat{\mathbf{H}}\hat{\mathbf{H}}}^{-1} \mathbf{r}_{f,v}, \quad (15)$$

where  $\mathbf{r}_{f,v} = E[\hat{\mathbf{H}}_j H_{j',v}^*]$  is the  $v$ th column of the cross-correlation matrix  $\mathbf{R}_{\hat{\mathbf{H}}\mathbf{H}}$ .

After FDCTF estimation filtering of the past FDCTFS in the MMSE sense,  $\hat{H}_{j,v}$  can be expressed as

$$\hat{H}_{j,v} = H_{j,v} + \zeta_{j,v}, \quad (16)$$

where  $\zeta_{j,v}$  is a zero-mean process having a variance of  $J_{fo(j,v)}$ , which represents the estimation error between  $\hat{H}_{j,v}$  and  $H_{j,v}$ . Based on the property that  $\zeta_{j,v}$  is independent of both  $\hat{H}_{j,v}$  and  $H_{j,v}$ , provided that we have  $j \neq j'$  [15], the autocorrelation function of  $\hat{H}_{j,v}$  at a given frequency can be expressed as:

$$E[\hat{H}_{j,v} \hat{H}_{j',v'}^*] = r_t[\Delta j] r_f[0] + J_{fo(j,v)} \delta(\Delta j). \quad (17)$$

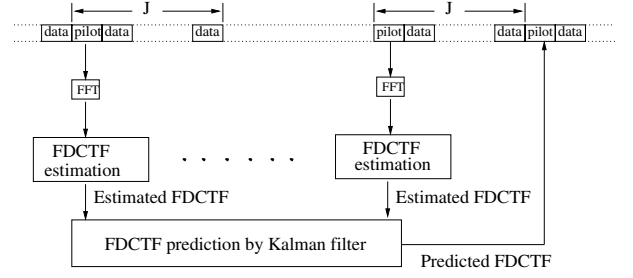


Fig. 2. Illustration of long range prediction for narrowband systems.

#### IV. CHANNEL PREDICTION AND INTERPOLATION

In this contribution we assume that a dedicated pilot OFDM/MC DS-CDMA symbol block having the same number of symbols as the data symbol block is inserted before every  $J - 1$  transmission blocks and the  $J$  consecutive transmission blocks are treated as a pilot-aided transmission frame in this investigation. As portrayed in Fig.2, the FDCTF associated with the next OFDM/MC DS-CDMA pilot symbol block is predicted with the aid of all the pilot blocks available from the past by invoking long-range prediction. As described in Section I, the FDCTF  $H_{j,v}$  experiences narrowband fading at a given subcarrier, provided that the bandwidth of each subcarrier is lower than the coherence bandwidth of the channel. Thus, a set of  $V$  Kalman filters can be used for predicting the future FDCTFs at each of the  $V$  subcarriers.

For a given FD subcarrier  $v$ ,  $v = 1, 2, \dots, V$ , the FDCTF can be described by an AR model [18], which is given by

$$H_{j,v} = \sum_{p=1}^P a_p H_{j-p,v} + w_{j,v}, \quad (18)$$

where  $\{a_p\}$  represents the AR coefficients derived in [18] and  $w_{j,v}$  is the AWGN.

According to [17], the Kalman filtering process used for predicting the FDCTF from all the past values on a subcarrier basis is formulated as

$$\check{\mathbf{H}}_{j,v} = \mathbf{F}_{j-1,v} \check{\mathbf{H}}_{j-1,v} + \mathbf{w}_{j,v}, \quad (19)$$

where we have  $\check{\mathbf{H}}_{j,v} = [H_{j,v}, H_{j-1,v}, \dots, H_{j-P+1,v}]^T$  and  $\mathbf{w}_{j,v} = [w_{(j,v)}, 0, \dots, 0]^T$  is the  $(P \times 1)$ -dimensional process noise vector. In Eq.(19),  $\mathbf{F}_{j-1,v}$  is the  $(P \times P)$ -dimensional transition matrix from time  $j - 1$  to  $j$  [17], which is given by

$$\mathbf{F}_{j-1,v} = \begin{bmatrix} a_1 & \dots & a_{P-1} & a_P \\ 1 & \dots & 0 & 0 \\ \vdots & \ddots & \vdots & \vdots \\ 0 & \dots & 1 & 0 \end{bmatrix}. \quad (20)$$

Furthermore, according to Eq.(16) the Kalman measurement equation [17] can be formulated as

$$\hat{H}_{j,v} = \mathbf{C}_{j,v} \check{\mathbf{H}}_{j,v} + \zeta_{j,v}, \quad (21)$$

where  $\mathbf{C}_{j,v} = [1, 0, \dots, 0]$  is a  $(1 \times P)$ -dimensional measurement matrix. Consequently, the Kalman filter based FDCTF prediction can be formulated as [17]

$$\hat{\mathbf{H}}_{[(j+1,v)|(j,v)]} = \mathbf{F}_{j,v} \hat{\mathbf{H}}_{[(j,v)|(j-1,v)]} + \mathbf{G}_{(j,v)} \boldsymbol{\alpha}_{j,v}, \quad (22)$$

where  $\hat{\mathbf{H}}_{[(j+1,v)|(j,v)]}$  represents the MMSE prediction of  $\check{\mathbf{H}}_{j+1,v}$  based on all the  $j$  observations of past pilot symbol blocks for a specific subcarrier, while  $\mathbf{G}_{j,v}$  and  $\boldsymbol{\alpha}_{j,v}$  are the Kalman gain and the

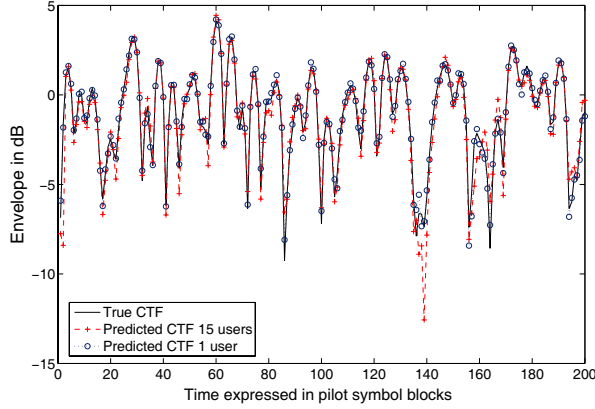


Fig. 3. The true CTF magnitude and the Kalman filter based predicted CTF magnitude of the 16th subcarrier, when assuming that the spacing of pilot symbol blocks was  $J = 30$  transmission blocks, the maximum Doppler frequency was  $f_{dm} = 100\text{Hz}$ , the transmission block duration was  $T_B = 0.00004\text{s}$ , the number of multipath components was  $L = 5$ , the length of the transmission block was  $M = 10$ , the length of the cyclic prefix was  $L - 1 = 4$ , the power intensity was  $\sigma_\ell^2 = 0.2$  for each multipath component and we had  $E_b/N_0 = 25\text{dB}$ . Furthermore, the order of the Kalman filter was  $P = 20$ .

innovation process, respectively [17]. According to [18], we have  $\mathbf{F}_{j,v} = \mathbf{F}_{j-1,v}$  in our investigations.

After long range FDCTF prediction, we attain the specific CTF corresponding to the data symbol block to be demodulated by interpolating the CTF over  $\mathcal{K}$  number of consecutive pilot symbol blocks. In [19], a sinc interpolator was proposed for conventional single-carrier modulation, where the fading amplitude of the  $j$ th data symbol in the  $n$ th transmitted frame was estimated from the  $\mathcal{K}$  number of surrounding pilot symbols, including the pilot symbols of the  $(\mathcal{K} - 1)/2$  previous frames, the current frame and of the  $(\mathcal{K} - 1)/2$  subsequent frames, which were predicted in advance by using Kalman filtering assisted FDCTF prediction. In this spirit, the estimate of the FDCTF  $\hat{H}_n^j$  corresponding to the  $j$ th MC DS-CDMA data symbol block in the  $n$ th MC DS-CDMA frame seen in Fig.2 may be expressed as [19]

$$\hat{H}_n^j = \sum_{k=-\lfloor(\mathcal{K}-1)/2\rfloor}^{\lfloor\mathcal{K}/2\rfloor} f_k^j \hat{H}_{n+k}^j, \quad (23)$$

where  $j = 1, \dots, J-1$  is the MC DS-CDMA data symbol block index between two pilot symbol blocks portrayed in Fig.2 while  $f_k^j$  denotes the real-valued interpolation coefficient, which is computed from the sinc function as

$$f_k^j = \text{sinc}\left(\frac{j}{J} - k\right). \quad (24)$$

## V. SIMULATION RESULTS

In this section we quantify the achievable performance of the generalized MC DS-CDMA system communicating over a  $L = 5$  paths dispersive Rayleigh fading channel contaminated by AWGN employing 15-chip Gold codes as TD spreading sequences and 32-chip Walsh codes as the FD spreading codes.

In Fig.3 the FD envelope of the true CTF  $H_{j,v}$  and its Kalman filter based FDCTF prediction  $\hat{H}_{[(j,v)|(j-1,n)]}$  are shown, when stipulating the assumption that the maximum Doppler frequency was

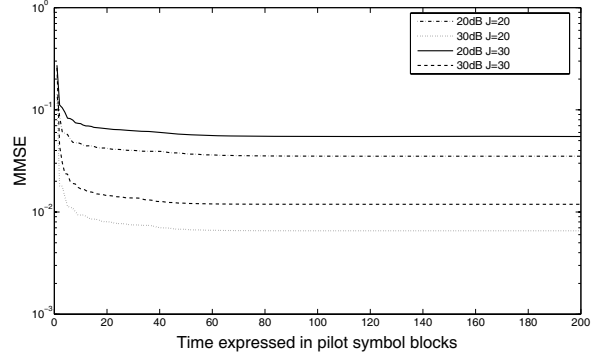


Fig. 4. The CTF MMSE versus the time expressed in terms of the number of the pilot symbol blocks for the Kalman filter based long-range FDCTF prediction of the 16th subcarrier, when assuming that the maximum Doppler frequency was  $f_{dm} = 100\text{Hz}$ , the transmission block duration was  $T_B = 0.00004\text{s}$ , the number of multipath components was  $L = 5$ , the length of transmission block was  $M = 10$ , the length of the cyclic prefix was  $L - 1 = 4$ , the power intensity was  $\sigma_\ell^2 = 0.2$  for each multipath component and the order of the Kalman filter was  $P = 20$ . In this simulation, we had both  $E_b/N_0 = 20\text{dB}$  and  $E_b/N_0 = 30\text{dB}$ . Furthermore, the spacing  $J$  of the pilot symbol block was assigned one of two different values: namely 20 and 30.

$f_{dm} = 100\text{Hz}$ , the number of multipath components was  $L = 5$ , the length of the pilot block was  $M = 10$ , the cyclic prefix was constituted by  $L - 1 = 4$  chips, the power intensity was  $\sigma_\ell^2 = 0.2$  for each of the  $L = 5$  multipath components, while the order of the Kalman filter was  $P = 20$ . Furthermore, we had  $E_b/N_0 = 25\text{dB}$  and the transmission block duration was  $T_B = 0.00004\text{s}$ , while the spacing of pilot symbol blocks was  $J = 30$ . We can observe from Fig.3 that when the SNR is sufficiently high, the Kalman filter based FDCTF predictor is capable of closely tracking the wideband channel's FDCTF. Furthermore, by employing multiuser decorrelating based channel estimation, the system supporting  $K = 15$  users achieved a near-single-user performance, since the MUI has been suppressed.

In Fig.4 we evaluated the achievable FDCTF MMSE performance versus the time expressed in terms of the number of the pilot symbol blocks used by for the Kalman filter based FDCTF predictor. In these investigations, we had  $E_b/N_0 = 20\text{dB}$  and  $E_b/N_0 = 30\text{dB}$ . All other parameters were the same as those in Fig.3. In Fig.4 the FDCTF MMSE associated with both  $J = 20$  and  $J = 30$  was recorded. Fig.4 demonstrates that the MMSE reaches a certain residual value, as the number of pilot symbol blocks used for Kalman filtering based prediction is increased. Moreover, for a fixed value of  $E_b/N_0$ , as expected the MMSE corresponding to  $J = 5$  is lower than that corresponding to  $J = 30$ .

In Fig.5 we evaluated the attainable FDCTF interpolation performance associated with different values of  $\mathcal{K}$ , when using  $J = 30$ . The FDCTF of pilot symbols were obtained according to Fig.3. Fig.5 shows that when supporting  $K = 4$  users, the system operating in conjunction with  $\mathcal{K} = 11$  outperformed that using  $\mathcal{K} = 7$  at the expense of a higher computational complexity. The system supporting  $K = 4$  users achieved a similar performance to that serving a single user, provided that they had the same value of  $\mathcal{K}$ .

Finally, the attainable BER performance of the systems carrying out FDCTF estimation, prediction and interpolation was comparatively investigated with that of the systems assuming perfect channel estimation. Fig.6 shows that when employing multiuser decorrelating detec-



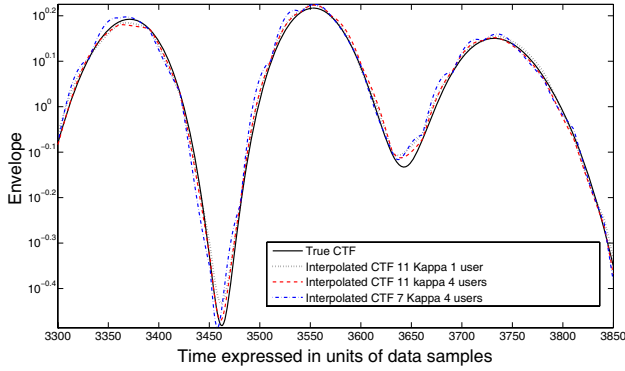


Fig. 5. The true CTF envelope and the interpolated CTF envelope for  $\mathcal{K} = 7$  and 11, when we had  $J = 30$ . The FDCTF was obtained by Kalman filtering assisted long range prediction, when assuming that the maximum Doppler frequency was  $f_{dm} = 100\text{Hz}$ , the transmission block duration was  $T_B = 0.00004\text{s}$ , the number of multipath components was  $L = 5$  and we had  $E_b/N_0 = 25\text{dB}$ . Furthermore, the order of the Kalman filter was  $P = 20$ .

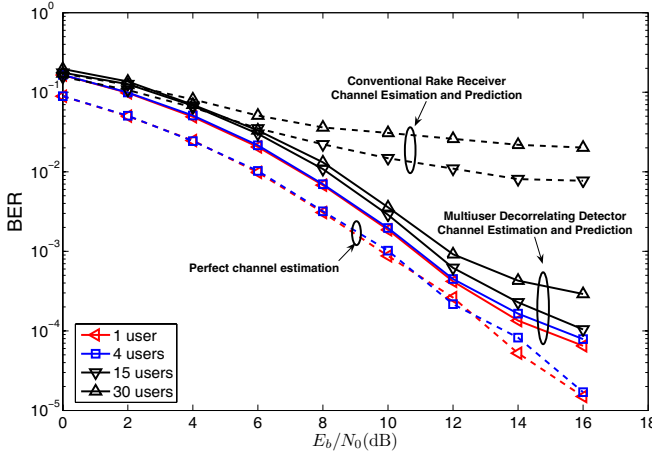


Fig. 6. BER versus  $E_b/N_0$  performance of the uplink of a generalized MC DS-CDMA wireless system operating in conjunction with  $\mathcal{K} = 11$  and  $J = 30$ . All other parameters were the same as those in Fig.5. In this simulation, the BER performance of the systems supporting different users were studied comparatively.

tors, the systems invoking FDCTF estimation, prediction and interpolation achieved a slightly worse BER performance than the systems assuming perfect channel estimation, i.e., about 1 dB worse at a BER of  $10^{-4}$ . Again, the system supporting  $K = 4$  users achieved a similar performance to that serving a single user. As expected, these systems outperformed that supporting  $K = 15$  or 30 users. Furthermore, Fig.6 suggested that the systems employing multiuser decorrelating detectors significantly outperformed the system refraining from multiuser decorrelating detection. These results confirmed that our multiuser decorrelating based channel estimator is robust to the effects of both the MUI and the background noise and hence improved the attainable BER performance.

## VI. CONCLUSIONS

In this contribution we have proposed a multiuser decorrelating based FDCTF estimation scheme designed for generalized MC DS-CDMA for the sake of estimating the FDCTFs associated with the pilot MC DS-CDMA symbols, which is capable of mitigating the effects of both the MUI and the background noise. Kalman filter assisted long range channel prediction was then carried out for predicting the future FDCTFs based on the current and previous pilot FDCTFs. Finally, we generated the FDCTFs for the data symbols by employing a sinc interpolator. Our simulation results demonstrated that Kalman filter based FDCTF predictor is capable of closely tracking the subcarriers' FD envelope at reasonable  $E_b/N_0$  values. Furthermore, the system supporting multiple users is capable of attaining a similar performance to the system serving a single user by invoking multiuser decorrelating based channel estimation.

## REFERENCES

- [1] L. Hanzo, L. L. Yang, E. L. Kuan, and K. Yen, *Single- and Multi-Carrier DS-CDMA*. John Wiley & Sons - IEEE Press, 2003, 1060 pages.
- [2] L. Hanzo, M. Munster, B. J. Choi, and T. Keller, *OFDM and MC-CDMA*. John Wiley & Sons - IEEE Press, 2003, 960 pages.
- [3] L. Vandendorpe, "Multitone spread spectrum multiple access communications system in a multipath Rician fading channel," *IEEE Transactions on Vehicular Technology*, vol. 44, no. 2, pp. 327-337, 1995.
- [4] E. A. Sourour and M. Nakagawa, "Performance of orthogonal multicarrier CDMA in a multipath fading channel," *IEEE Transactions on Communications*, vol. 44, pp. 356-367, March 1996.
- [5] Ramjee Prasad and Shinsuke Hara, "Overview of Multicarrier CDMA," *IEEE Communications Magazine*, pp. 126-133, Dec. 1997.
- [6] L.-L. Yang and L. Hanzo, "Performance of generalized multicarrier DS-CDMA over Nakagami- $m$  fading channels," *IEEE Transactions on Communications*, vol. 50, pp. 956-966, June 2002.
- [7] A. Duel-Hallen, S. Hu and H. Hallen, "Long range prediction of fading signals: enabling adaptive transmission for mobile radio channels," *IEEE Signal Processing Magazine*, vol. 17, pp. 62-75, May 2000.
- [8] J. K. Huang and J. H. Winters, "Sinusoidal modeling and prediction of fast fading processes," *Global Telecommunications Conference*, vol. 2, pp. 892-897, November 1998.
- [9] L. Dong, G. Xu and H. Ling, "Prediction of fast fading mobile radio channels in wideband communication systems," *Global Telecommunications Conference*, pp. 3287-3291, November 2001.
- [10] S. Semmelrodt and R. Kattenbach, "Application of spectral estimation techniques to 2-D fading forecast of time-variant channels," *COST 273 TD(01)034*, October 2001.
- [11] S. Semmelrodt and R. Kattenbach, "A 2-D fading forecast of time-variant channels based on parametric modelling techniques," *The 13th IEEE International Symposium on Personal, Indoor and Mobile Radio Communications*, pp. 1640-1644, September 2002.
- [12] T. Hwang and Y. Li, "Iterative cyclic prefix reconstruction for coded single-carrier systems with frequency-domain equalization (SC-FDE)," *IEEE Vehicular Technology Conference 2003-Spring*, pp. 1841-1845, April 2003.
- [13] Y. S. Choi and P. J. Voltz and F. A. Cassara, "On channel estimation and detection for multicarrier signals in fast and selective Rayleigh fading channels," *IEEE Transactions on Communications*, vol. 49, pp. 1375-1387, Aug. 2001.
- [14] S. Verdu, *Multuser Detection*. Cambridge University Press, 1998, 474 pages.
- [15] P. Hoehner, "A statistical discrete-time model for the WSSUS multipath channel," *IEEE Transactions on Vehicular Technology*, vol. 41, pp. 461-468, November 1992.
- [16] W. G. Jeon, K. H. Paik and y. S. Cho, "Two-dimensional MMSE channel estimation for OFDM systems with transmitter diversity," *IEEE Vehicular Technology Conference 2001-Fall*, pp. 1682-1685, October 2001.
- [17] S. Haykin, *Adaptive Filter Theory*. Prentice Hall, Inc, 2002.
- [18] K. E. Baddour and N. C. Beaulieu, "Autoregressive models for fading channel simulation," *IEEE Global Telecommunications Conference*, pp. 1187-1192, November 2001.
- [19] X. Y. Tang and M. S. Alouini and A. J. Goldsmith, "Effect of channel estimation error on M-QAM BER performance in Rayleigh fading," *IEEE Transactions on Communications*, vol. 47, pp. 1856-1864, Dec. 1999.